

The Prediction of the Wall Bounded Turbulent Flows Using the Code PASSABLE

Ertan BAYDAR, Burhan ÇUHADAROĞLU
*Karadeniz Technical University,
Department of Mechanical Engineering,
Trabzon-TURKEY*

Received 06.03.1997

Abstract

Turbulent flows for flat plate and circular pipes were solved using the two equation $k-\varepsilon$ model and the algebraic stress model (ASM). The computations were carried out using the parabolic solver PASSABLE code which uses a finite-difference and finite-volume approach with a forward marching technique. The results obtained with the code were compared with the results described in the literature and a good agreement was found.

Key Words: $k-\varepsilon$ turbulence model, algebraic stress model, flat plate flow, pipe flow

PASSABLE Programı ile Duvarla Sınırlı Türbülanslı Akışların Hesaplanması

Özet

Düzlem levha ve borudaki türbülanslı akışlar iki denklemlili $k-\varepsilon$ ve cebrik gerilme türbülans modelleri kullanılarak çözülmüştür. Hesaplamalar ileriye doğru çözüm tekniği ile sonlu fark ve sonlu hacim yaklaşımı kullanan parabolik tipte PASSABLE bilgisayar programı ile gerçekleştirilmiştir. Bu bilgisayar programı ile elde edilen sonuçlar mevcut deneysel sonuçlarla karşılaştırılmış ve iyi bir uyum sağlanmıştır.

Anahtar Sözcükler: $k-\varepsilon$ türbülans modeli, cebrik gerilme modeli, düzlem levha akışı, boru akışı

1. Introduction

The predictions of turbulent flows, which are of great practical importance, can be obtained using turbulence models. The main distinction between turbulence models is whether turbulence properties are related directly to the mean flow or obtained from a transport equation such as Reynolds transport equation. A wide variety of flows have been predicted with the $k-\varepsilon$ and algebraic stress with reasonable accuracy.

Ng and Spalding (1972) have predicted the

boundary layer flows near walls by means of a turbulence model which employs the turbulence energy, and the product of this energy with a length scale. Jones and Launder (1973) have calculated the fully-developed turbulent flow in a pipe with the $k-\varepsilon$ model. A simplified algebraic stress model was used by Lemos and Sesonske (1985) to investigate the turbulent flow of mercury in a pipe. Direct numerical simulations and experiments on fully-developed turbulent pipe flow for low Reynolds numbers have been

carried out by Egges et al. (1994). Spalart (1988) has studied the direct simulation of developing a turbulent boundary layer on a flat plate. Direct and large-eddy simulations of turbulence have been reviewed by Rogallo and Moin (1984). Kim and Chung (1988) and Yule et al. (1993) have applied the standard k - ε model and the algebraic stress model to turbulent jet flow. They have concluded that the algebraic stress model gave more accurate predictions than the k - ε model in terms of velocity components.

2. Turbulence models

The two-equation k - ε model, which specifies the turbulent viscosity, and the algebraic stress model (ASM), which takes into account the stress transport, were used in this study. Both models are based on modelled versions of exact transport equations for the Reynolds stresses and the rate of dissipation of turbulence energy.

k - ε

The Jones and Launder (1972) model, also known as the k - ε model, relates the distributions of the turbulence kinetic energy k and its rate of dissipation ε to an eddy viscosity. For the steady, incompressible flow, the distributions of k and ε were obtained from the solution of the following transport equations:

$$U_j \frac{\partial k}{\partial x_j} = \frac{\partial}{\partial x_j} \left[\left(\nu + \frac{\nu_t}{\sigma_k} \right) \frac{\partial k}{\partial x_j} \right] + \nu_t \left(\frac{\partial U_i}{\partial x_j} + \frac{\partial U_j}{\partial x_i} \right) \frac{\partial U_i}{\partial x_j} - \varepsilon \quad (1)$$

$$U_j \frac{\partial \varepsilon}{\partial x_j} = \frac{\partial}{\partial x_j} \left[\left(\nu + \frac{\nu_t}{\sigma_\varepsilon} \right) \frac{\partial \varepsilon}{\partial x_j} \right] + C_{\varepsilon 1} \frac{\varepsilon}{k} \nu_t \left(\frac{\partial U_i}{\partial x_j} + \frac{\partial U_j}{\partial x_i} \right) \frac{\partial U_i}{\partial x_j} - C_{\varepsilon 2} \frac{\varepsilon^2}{k} \quad (2)$$

where $\nu_t = C_\mu k^2 / \varepsilon$ and $\varepsilon = k^{3/2} / l$. l is the turbulence length scale. The model constants are $\sigma_k=1$, $\sigma_\varepsilon=1.25$, $C_{\varepsilon 1}=1.44$, $C_{\varepsilon 2}=1.92$ and $C_\mu=0.09$ (Launder and Spalding, 1974).

The algebraic stress model (ASM)

The ASM is a procedure for solving transport equations for all individual Reynolds stresses. Launder et al. (1975) have assumed proportionality between the net transport of each stress and the corresponding transport of k , which yields

$$\frac{u_i \bar{u}_j}{k} (P_k - \varepsilon) = (1 - C_2) P_{ij} + \frac{2}{3} C_2 \delta_{ij} P_k - C_1 \frac{\varepsilon}{k} u_i \bar{u}_j + \frac{2}{3} (C_1 - 1) \delta_{ij} \varepsilon \quad (3)$$

where the production rate of k is defined by $P_k = -u_i \bar{u}_j (\partial U_i / \partial x_j)$. P_{ij} is the rate of production tensor of $u_i \bar{u}_j$ and δ_{ij} is a Kronecker delta. The model constants are $C_1=1.8$ and $C_2=0.6$ (Gibson, 1978).

Both models used in this study are valid for high Reynolds number flows, away from viscous near-wall regions only, ignoring the effects of fluid viscosity on turbulence. It thus follows that wall-bounded flows require special treatment near the wall to account for viscous-sublayer effects. In particular, the wall shear stress, the near-wall generation and dissipation of turbulence energy need to be considered. As a description of the wall function (Schlichting, 1979), the non-dimensional wall distance was defined $y^+ = y U_\tau / \nu$ where U_τ is a friction velocity. In our computation, it was assumed that at $y^+ \geq 30$ viscous effects were negligible and that within $y^+ < 30$ momentum transport could be ignored.

3. Numerical Procedure

The general equations for steady axisymmetric flow of the boundary-layer type reduce to the following forms:

continuity:

$$\frac{\partial \rho U}{\partial x} + \frac{1}{r} \frac{\partial \rho r V}{\partial r} = 0 \quad (4)$$

momentum:

$$\frac{\partial \rho U^2}{\partial x} + \frac{1}{r} \frac{\partial r \rho U V}{\partial r} = -\frac{\partial P}{\partial x} + \frac{1}{r} \frac{\partial}{\partial r} \left(r \mu \frac{\partial U}{\partial r} - r \rho \overline{uv} \right) \quad (5)$$

$$\frac{\partial \rho U \phi}{\partial x} + \frac{1}{r} \frac{\partial r \rho V \phi}{\partial r} = -\frac{1}{r} \frac{\partial}{\partial r} \left(-r \Gamma_\phi \frac{\partial \phi}{\partial r} + r \rho \overline{\phi v} + S_\phi \right) \quad (6)$$

Equation 6 can represent Equations 1 or 2 by choosing $\phi=k$ and $\phi = \varepsilon$, respectively, and inserting gradient diffusion models for \overline{kv} and $\overline{v\varepsilon}$.

The PASSABLE code of Leschziner (1981) was used in this study. The code solved the governing equations in a forward marching manner. At any stage of the solution, upstream conditions were used to obtain the flow conditions on a single downstream

plane. Discretization was based on the fully conservative finite-volume approach. Second-order central differences were used to approximate the cross-flow convection and diffusion terms. The formulation was implicit in the streamwise direction. The code solved discretized versions of the partial differential equations governing the transport of momentum and any relevant intensive scalar properties over a domain whose width generally varied with downstream distance. The numerical mesh was such that a fixed number of mesh lines covered the width of the flow field whether this width was constant or variable with the streamwise direction. The mesh was non-orthogonal in general, reverting to a Cartesian or a polar cylindrical system when the width of the flow field was held constant. The method adopted in the code was to transform the governing equations from the (x,y) to an (ξ,η) system, as the flow over a flat plate shown in Figure 1. Our procedure was forward marching one, advancing the solution from any upstream to a following downstream station. Figure 2 shows the numerical mesh and associated control volumes within a forward step. The main control volume relating to the axial velocity component U and any scalar (P, k and ε) is shown in Figure 2a. The faces η_+ and η_- bisect co-responding internodal distances. As shown in Figure 2b, the radial velocity component V was staggered midway between nodal locations P_j and P_{j-1} , which had advantages for the

formulation of the continuity equation from which V was obtained. The hybrid difference scheme (HDS) was used for the momentum equations (Patankar, 1980).

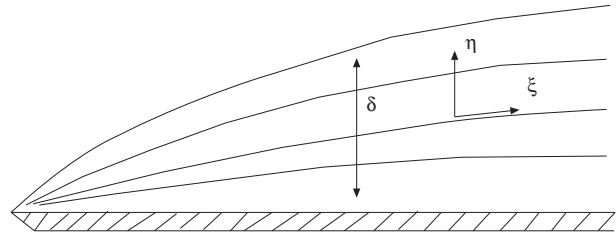


Figure 1. The ξ, η coordinate system

The solution of the momentum equation required knowledge of the pressure gradients. The treatment in the code initially used the pressure gradient of the upstream station. This resulted in a velocity distribution that would not necessarily satisfy overall mass conservation. The aim was therefore to iterate and reduce the amount of mass flux imbalance. The finite-difference equations for the variables U, k and ε were solved using the tridiagonal matrix algorithm. Approximately 16 nodes across the flow, from the centerline, were found to give grid-independent solutions. All computations for pipe flow were carried out using approximately 4450 steps downstream.

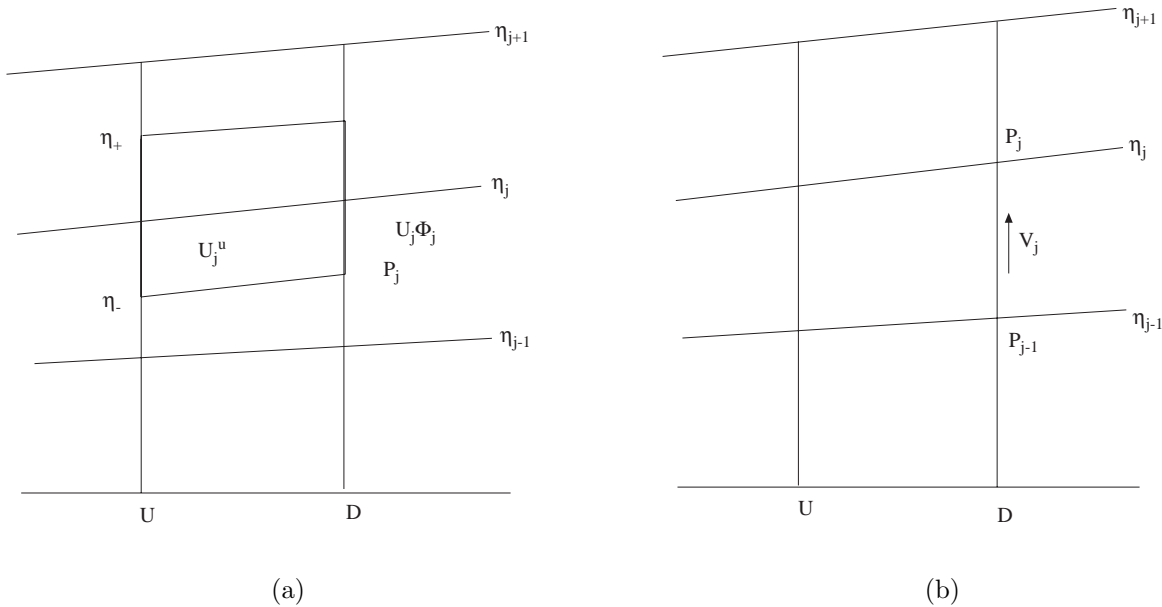


Figure 2. Numerical mesh and control volumes a) U -momentum and scalars; b) V -momentum

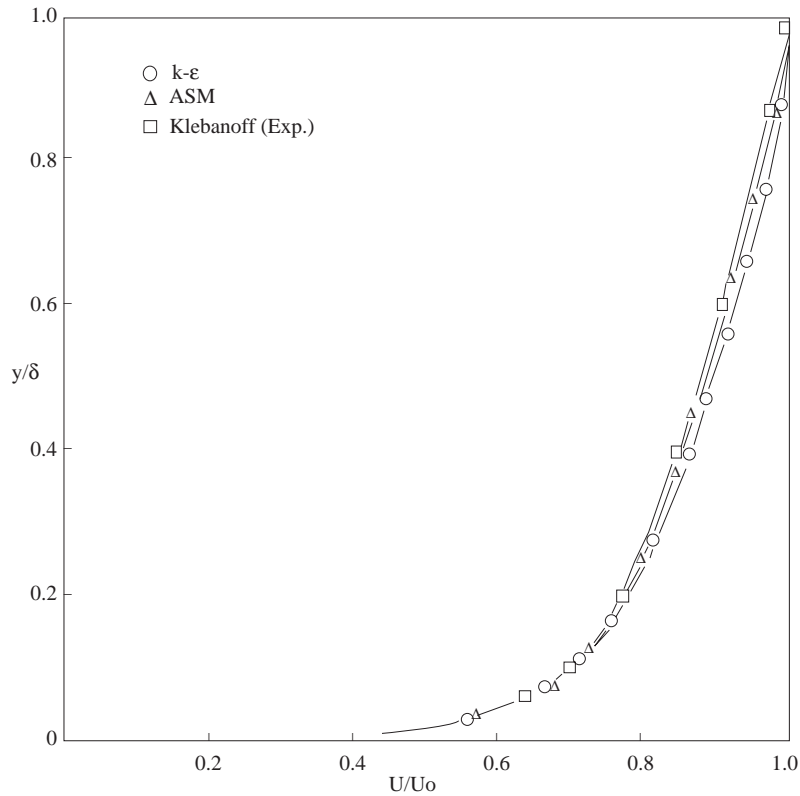


Figure 3. Axial mean velocity profiles on the flat plate

4. Results

The computations were performed with an algebraic stress model and the standard $k-\epsilon$ model for predictions of mean velocity and turbulence kinetic energy in the flow field of a flat and a circular pipe. The results were compared with Klebanoff's (from Ng and Spalding, 1972) and Laufer's (from Jones and Launder, 1973).

Flat plate

The initial values of the velocity and turbulence kinetic energy were uniform and equal to 10 m/s and $0.0001 \text{ m}^2/\text{s}^2$, respectively. The plate length was 6.5 m. The upper boundary of solution domain was expanded in the streamwise direction appropriate to the parabolic nature of the flow over the flat plate. The boundary layer thickness was 0.1133 m at $x=6.294$ m from the leading edge of the plate. The Reynolds number, based on free stream velocity and boundary layer thickness, was 7.5×10^4 . This value also corresponded with a Reynolds num-

ber of 3.94×10^6 calculated from the free stream velocity and downstream distance. Figure 3 shows the comparison between the velocity profiles predicted with the $k-\epsilon$ model and ASM at $x=6.294$ m for flow over a flat plate and shows the experimental data of Klebanoff. The agreement seems very good. The predictions of turbulence kinetic energy in the boundary layer along the flat plate are given in Figure 4, together with Klebanoff's. The prediction values at $y/\delta > 0.2$ for k are slightly larger than the experimental data. It can be seen that the results obtained from the $k-\epsilon$ model are close to the experimental data. Figure 5 shows the variation in the skin friction coefficient along the flat plate. Also shown are the results obtained by Coles and Hirst (1968) from the data of Wiegardt and the results of Prandtl's theoretical formula defined as $C_f=0.0592Re^{-0.2}$ (Schlichting, 1979). The predictions obtained with the $k-\epsilon$ model and ASM showed only small discrepancies. After $x=3$ m, the predictions agree well with Prandtl's theoretical formula.

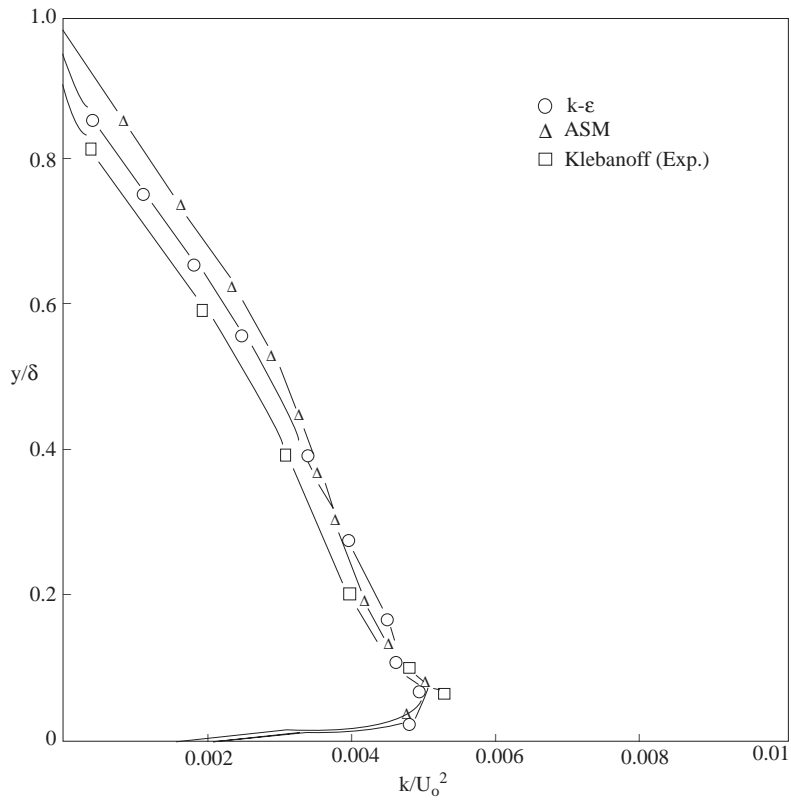


Figure 4. Kinetic energy profiles on the flat plate

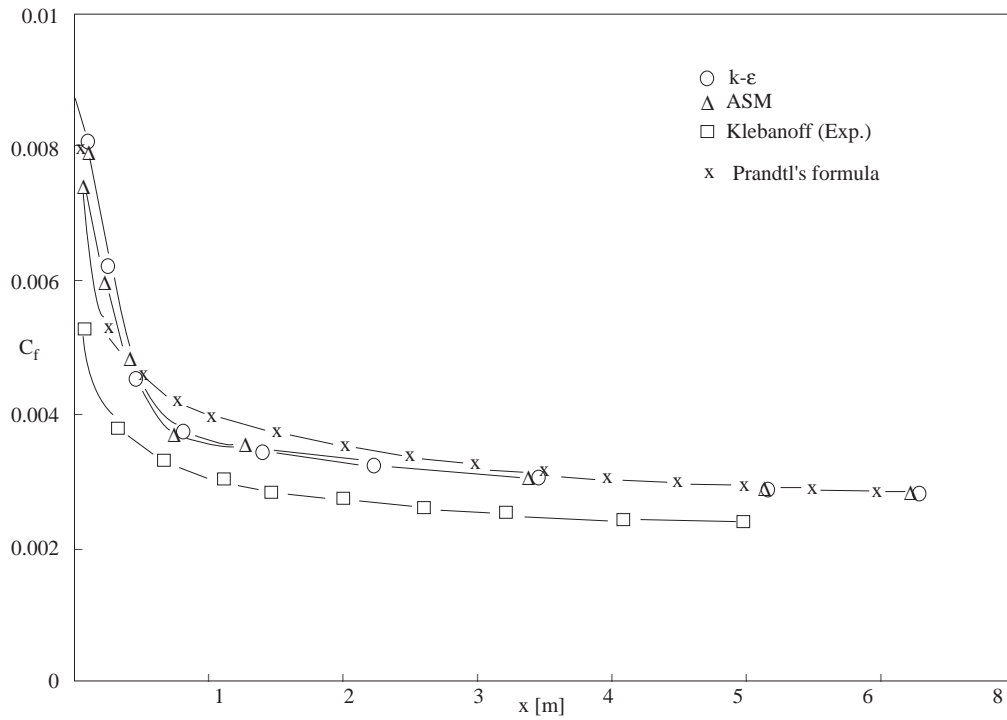


Figure 5. Distribution of skin friction coefficients along the flat plate

circular pipe

The length and diameter of the pipe were $L=7.2$ m and $D=0.18$ m. The inlet profiles for the velocity and turbulence kinetic energy were uniform. The inlet velocities were 4.2 m/s and 42 m/s for $Re=50000$ and $Re=500000$, respectively. The initial turbulence kinetic energy was $0.0001 \text{ m}^2/\text{s}^2$. The variation of the entrance length of the flow to the Reynolds number is given in Figure 6 for the $k-\varepsilon$ model and ASM. As the Reynolds number increased, the entrance length also increased. It can be seen that the values predicted with ASM were slightly higher than those of the $k-\varepsilon$ model.

Figures 7a and b show the velocity profiles predicted with the $k-\varepsilon$ model and ASM for various Reynolds numbers in the developed flow region. These profiles compare with Laufer's results. For $Re=50000$, the predictions coincide with each other and agree with the experimental data (Figure 7a). The predictions of ASM are closer to the experimental data for $Re=500000$ (Figure 7b).

The kinetic energy profiles predicted with the $k-\varepsilon$

model and ASM are compared in Figures 8a and b for $Re=50000$ and 500000 , respectively. There were discrepancies between the predictions and the results, but there were only small discrepancies in the region near the wall. Furthermore, the $k-\varepsilon$ model predicted lower values than the ASM for the region near the wall.

5. Conclusions

This research was primarily concerned with the accuracy and economics of the PASSABLE computer code which incorporated the turbulence models of standard $k-\varepsilon$ and algebraic stress. The results for the considered flows in turbulence models in code had only small discrepancies and were in agreement with experiments except for the kinetic energy profiles. Because the code solve the governing equations in a forward marching manner which allows a one-dimensional storage of all dependent variables, it is highly economical.

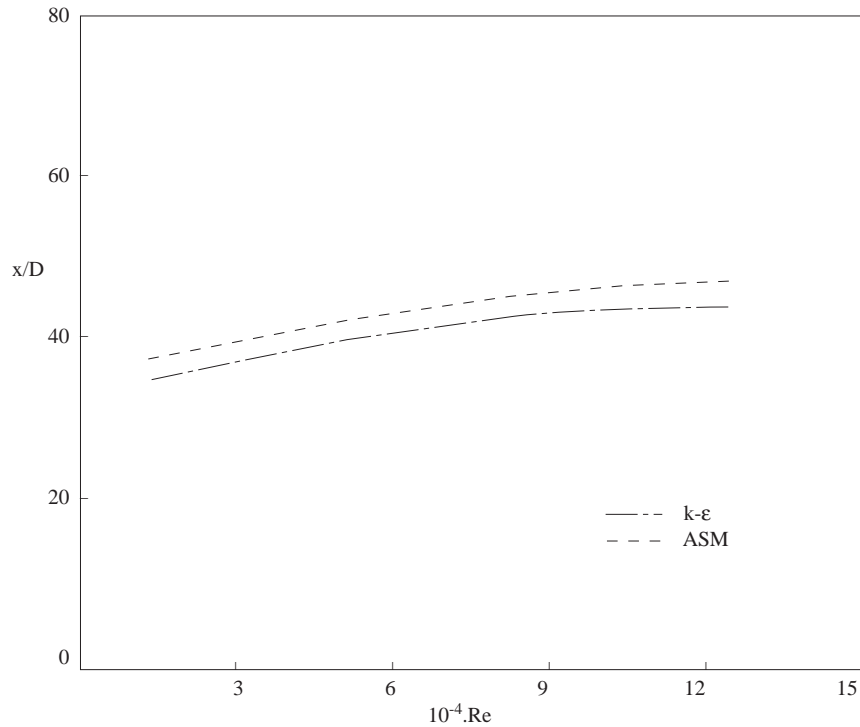


Figure 6. The entrance length in the pipe flow

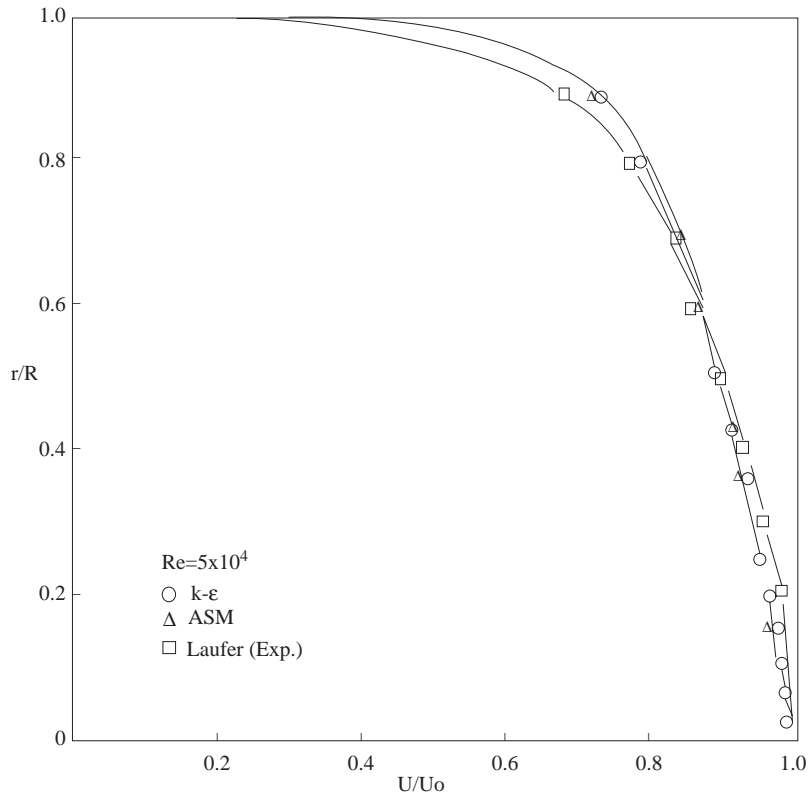


Figure 7a. Axial mean velocity profiles in the pipe flow a) $Re=5 \times 10^4$

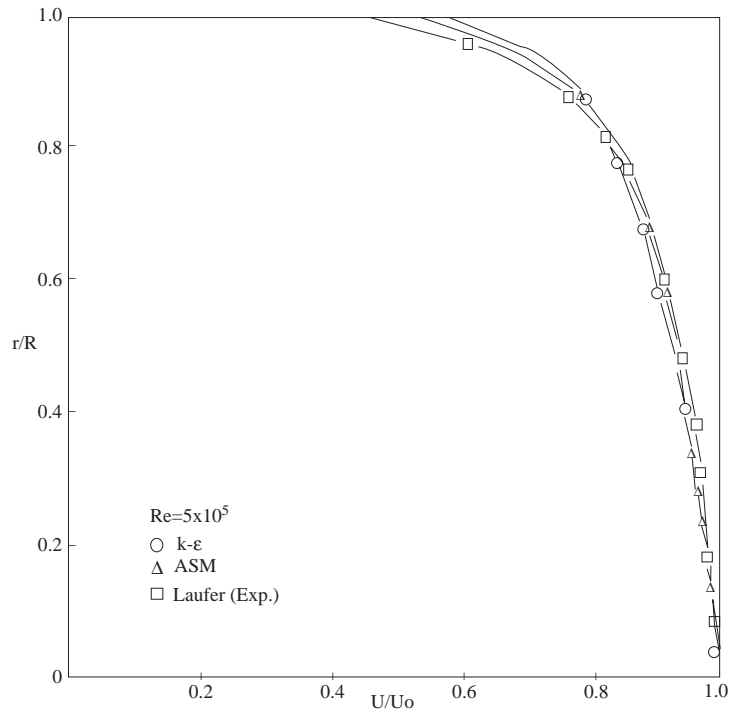


Figure 7b. Axial mean velocity profiles in the pipe flow a) $Re=5 \times 10^5$

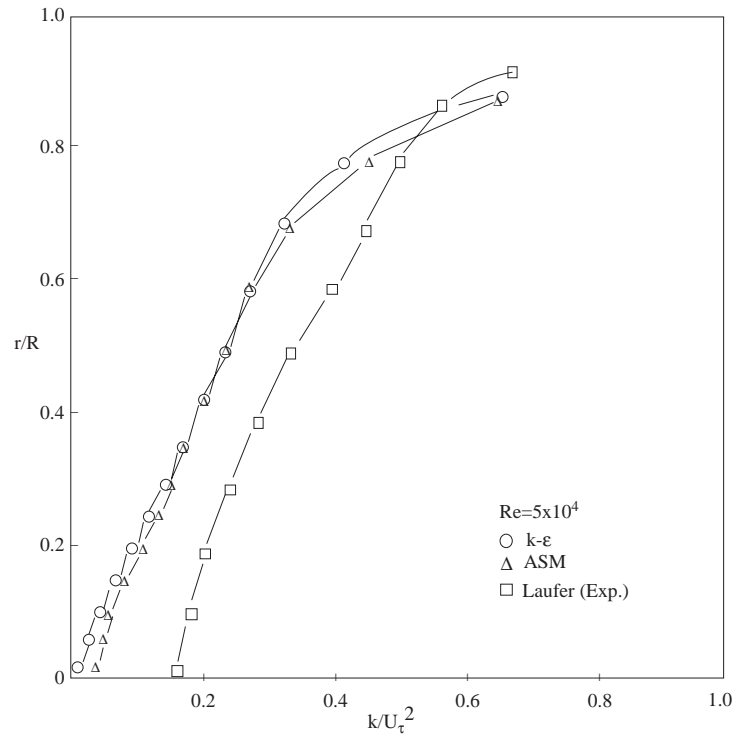


Figure 8a. Kinetic energy profiles in the pipe flow a) $Re = 5 \times 10^4$

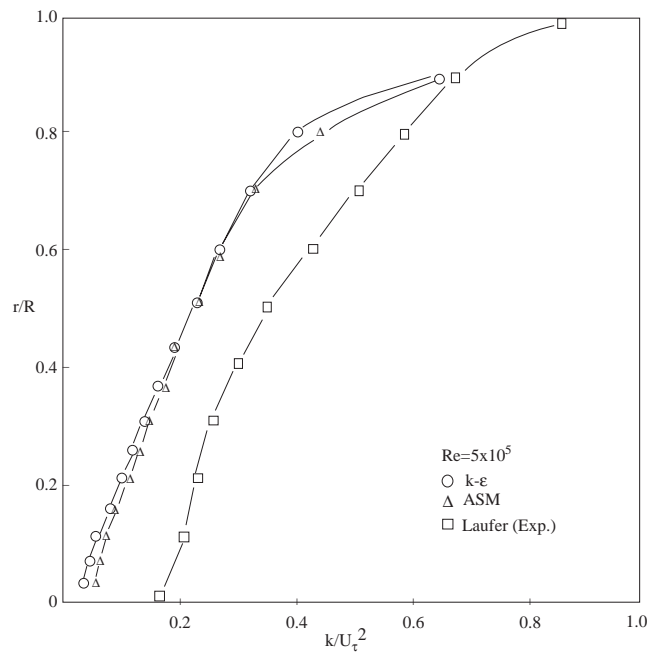


Figure 8b. Kinetic energy profiles in the pipe flow a) $Re = 5 \times 10^5$

C_f	: Skin friction coefficient	U_0	: Free stream or centerline mean velocity
D	: Pipe diameter	U_τ	: Friction velocity
k	: Turbulent kinetic energy, $u_i \bar{u}_i / 2$	V	: Mean velocity component in radial direction
l	: Turbulence length scale	x	: Axial distance
L	: Length of the plate or pipe	y	: Distance from wall
r	: Radial distance	y^+	: Dimensionless wall coordinate
R	: Pipe radius	σ	: Boundary layer thickness
u_i	: Fluctuating velocity component in x_i direction	ε	: Rate of dissipation of k
U	: Mean velocity component in axial direction	ν	: Kinematic viscosity

References

- Coles D.E. and Hirst E.A., "Vol II, Compiled Data", Proceedings Computation of Turbulent Boundary Layers, AFOSR-IFP-Stanford Conference, 1968.
- Eggels J.G.M., Unger F., Weis M.H., Westerweel J., Adrian R.J., Friedrich R. and Nieuwstadt F.T.M., "Fully-Developed Turbulent Pipe Flow A Comparison between Direct Numerical Simulation and Experiment", J. Fluid Mech. 268, 175-209, 1994.
- Gibson M.M., "An Algebraic Stress and Heat-Flux Model for Turbulent Shear Flow with Streamline Curvature", Int. J. Heat Mass Transfer, 21, 1609-1617, 1978.
- Jones W.P. and Launder B.E., "The Prediction of Laminarization with a Two Equation Model of Turbulence", Int. J. Heat Mass Transfer, 15, 301-140, 1972.
- Jones W.P. and Launder B.E., "The Calculation of Low Reynolds Number Phenomena with a Two Equation Model of Turbulence", Int. J. Heat Mass Transfer, 16, 1119-1130, 1973.
- Kim K.Y. and Chung M.K., "Calculation of a Strongly Swirling Turbulent Round Jet with Recirculation by an Algebraic Stress Model", Int. J. Heat and Fluid Flow, 9, 62-68, 1988.
- Launder B.E., Reece G.J. and Rodi W., "Progress in the Development of a Reynolds Stress Turbulent Closure", J. Fluid Mech. 68, 537-566, 1975.
- Launder B.E. and Spalding D.B., "The Numerical Computation of Turbulent Flow", Comp. Meth. Appl. Mech. Eng. 3, 269-289, 1974.
- Lemos M.J.S. and Sesonske A., "Turbulence Modeling in Combined Convection in Mercury Pipe Flow", Int. J. Heat Mass Transfer, 28, 1067-1088, 1985.
- Leschziner M.A., "PASSABLE: A Computer Code for Parabolic Type Turbulent Flows", Department of Mechanical Engineering, UMIST, Manchester UK (internal report), 1981.
- Ng K.H. and Spalding D.B., "Turbulence Model for Boundary Layers near Walls", The Physics of Fluids, 15, 20-30, 1972.
- Patankar S.V., "Numerical Heat Transfer and Fluid Flow", McGraw-Hill, 1980.
- Rogallo R.S. and Moin D., "Numerical Simulation of Turbulent Flows", Ann. Rev. Fluid Mech. 16, 99-138, 1984.
- Schlichting H., Boundary-Layer Theory, 7th Ed., McGraw-Hill, 1979.
- Spalart P.R., "Direct Simulation of a Turbulent Boundary Layer up to $Re_\theta=1410$ ", J. Fluid Mech. 187, 61-98, 1988.
- Yule A.J., Damou M. and Kostopoulos D., "Modeling Confined Jet Flow", Int. J. Heat and Fluid Flow, 14, 10-17, 1993.